

Predictions of elastic alpha particle scattering from theoretical nuclear densities

A. M. Bernstein, B. H. Cottman, and P. Dick*

Physics Department and Laboratory of Nuclear Science, Massachusetts Institute of Technology, Cambridge, Massachusetts 02139

C. N. Papanicolas

Physics Department and Nuclear Physics Laboratory, University of Illinois at Urbana-Champaign, Urbana, Illinois 61801

(Received 26 April 1985)

Data for the diffraction region of the elastic scattering of 42–140 MeV α particles from $^{42,44,48}\text{Ca}$ have been compared to calculations based on Hartree-Fock nuclear densities. The α -particle optical potential was obtained from the densities using a double folding model where the effective interaction was adjusted to the scattering from ^{40}Ca . This study is insensitive to the details of the reaction calculation because it is restricted to the diffraction region and is only for the purpose of comparing relative sizes. The predicted cross section is in good agreement with data indicating that the theoretical densities are correct in the vicinity of 10% of central density to approximately ± 0.1 fm. This uncertainty is dominated by the approximations in the reaction calculation.

I. INTRODUCTION

During the past few years a good level of agreement between theoretical nuclear charge densities^{1,2} and those reconstructed from electron scattering data has been achieved.^{3–5} Throughout the nuclear periodic table, the agreement is almost perfect in the surface region with small but significant discrepancies persisting in the interior. One would expect that theoretical calculations which reproduce the proton densities should also reasonably predict the neutron densities, since the neutron-proton interaction is approximately three times the neutron-neutron or proton-proton interactions.

Hadronic probes are sensitive to both the neutron and proton distributions. However, the accuracy of the reaction calculation is not as good as for electron scattering. To a considerable extent all hadronic probes are limited by model errors, and the final justification of their use in extracting matter densities lies in the consistency of their results. A balanced review and extensive references are given in Ref. 6. The usual meeting ground between experiment and Hartree-Fock calculations has been a comparison of rms radii and density distributions. Recently it has been shown⁷ that the rms matter radii of medium-heavy nuclei relative to ^{40}Ca are in agreement for a wide variety of hadronic probes. In the same work⁷ it was shown that the predicted rms radii from ^{40}Ca to ^{68}Zn are in reasonable agreement with the data.

In this paper we will explore the sensitivity of the α probe to the nuclear surface by comparing experimental cross sections with those predicted using Hartree-Fock densities. Only the diffraction scattering region was utilized, as the cross sections are large and multistep contributions are relatively small in this region.

II. REACTION MODEL

The diffraction region of the α -particle elastic scattering cross sections are calculated using a double folding

model.^{8,9} This relates the ground state matter density $\rho(r)$ of the target nucleus to the scattering cross section through the α -nucleus optical potential $U(r_\alpha)$. In this model $U(r_\alpha)$ is postulated to be proportional to the convolution of $\rho(r)$ with a local effective α -nucleon interaction:

$$V_{\text{eff}}(r-r_\alpha) = V_0 f(r-r_\alpha),$$

$$U(r_\alpha) = V_0 (1+i\xi) \int \rho(r) f(r-r_\alpha) dr, \quad (1)$$

where V_0 and ξ are empirical functions of E_α , the α -particle energy,¹⁰ which correct the lowest order expression for the optical potential.¹¹

A simple geometric estimate of V_{eff} has been made by calculating the spatial, spin, and isospin average of the low energy nucleon-nucleon interaction and the α -particle density as measured by electron scattering. Both were taken to be of the Gaussian form which results in V_0 of 37 MeV and

$$f(r-r_\alpha) = \exp \left[- \left[\frac{r-r_\alpha}{r_0} \right]^2 \right], \quad (2)$$

with r_0 of approximately 2.0 fm.¹² It is a simplification to replace a nonlocal, energy- and density-dependent operator^{11,13,14} by the local interaction $U(r_\alpha)$ given in Eq. (1). The underlying nuclear dynamics are known to be highly complex and beyond our current calculational capabilities. In this respect the above simple folding model can only be justified on the basis of its success in describing known systems. The applicability of the model has been tested by successfully predicting the observed α -particle cross sections for $N=Z$ nuclei using densities determined from electron scattering.⁸ We believe that this success is due to the fact that only the diffraction scattering regime has been employed. The most accurate use of this model is in determining relative nuclear sizes (e.g., isotopic differences about doubly closed shell nuclei).

TABLE I. Values of scattering model parameters. The assumed theoretical Hartree-Fock ^{40}Ca densities are DDHF (Ref. 1) and DME (Ref. 2). The parameters given here are the ones with constant range parameter, $r_0 = 1.86$ fm for the DDHF density and $r_0 = 1.91$ fm for the DME density.

E_α (MeV)	^{40}Ca density	$V_0/37$ MeV	ξ
42.6	DDHF	1.20 ± 0.05	0.34 ± 0.06
79.1	DDHF	1.20 ± 0.08	0.49 ± 0.05
104.0	DDHF	0.97 ± 0.04	0.60 ± 0.03
142.0	DDHF	0.98 ± 0.08	0.52 ± 0.05
42.6	DME	1.36 ± 0.05	0.34 ± 0.05
79.1	DME	1.35 ± 0.11	0.48 ± 0.08
104.0	DME	1.09 ± 0.04	0.60 ± 0.03
142.0	DME	1.10 ± 0.11	0.53 ± 0.05

The parameters of the model (V_0, ξ , and r_0) were adjusted to reproduce the α -particle scattering from ^{40}Ca , the heaviest stable $N=Z$ nucleus. The matter distribution is well known since the neutron density, $\rho_n(r)$, is approximately equal to the proton density, $\rho_p(r)$. The Hartree-Fock densities for ^{40}Ca were used to determine the α -scattering model parameters. With this as a basis, the folding model is sensitive to density differences relative to ^{40}Ca .

The adjustable parameters of the effective interaction are assumed to be target independent. At each energy the parameters were determined through a χ^2 fit to the ^{40}Ca data. Only the first three maxima of the diffractive pattern were taken into account given that the applicability and reliability of this model have been demonstrated only in this region.

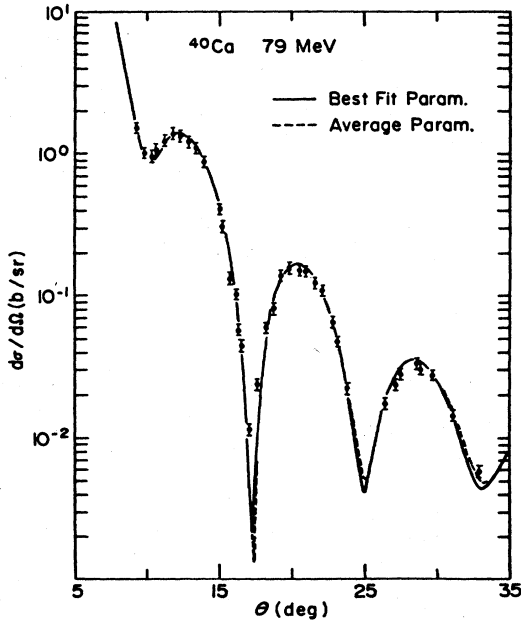


FIG. 1. Fits obtained for the scattering of 79 MeV α particles for our calibration nucleus ^{40}Ca . Both theoretical densities produce indistinguishable results. The solid curve is obtained by adjusting the three reaction model parameters. The dashed curve shows the best fit when the range parameter r_0 is kept fixed for all energies.

For ^{40}Ca the Hartree-Fock density matrix expansion (DME) of Negele and Vautherin² and the density dependent Hartree-Fock-Bogoliubov (DDHF) densities of Decharge and Gogny¹ were used. At each energy the three model parameters, V_0 , ξ , and r_0 , were determined for each density. It was observed that the range parameter, r_0 , varied by less than 10% over the energy region studied here. Therefore, for simplicity a parameter set with an average range was determined for each HF density. These parameters are presented in Table I. They exhibit the same systematic behavior found in an earlier work.¹⁰ The empirical values of the parameters are found to be close to the simple geometrical estimates.¹² The errors presented in Table I were estimated by increasing each parameter independently until χ^2 increased by 50% above the best fit value, which was found to give a reasonable representation of the model error.⁷

Both reaction parameter sets and both HF densities produce equally good agreement with the 79 MeV experimental data,¹⁵ as is illustrated in Fig. 1. In Fig. 2 the ^{40}Ca results for 42 MeV (Ref. 7), 104 MeV (Ref. 14), and 140 MeV (Ref. 16) data are shown. Good agreement between the reaction model and experiment is found at all energies. The densities from the two HF theories for ^{40}Ca produce almost indistinguishable differential cross sections at all energies.

III. THE Ca ISOTOPES

For $^{42,44,48}\text{Ca}$ the HF densities were used with the folding model to predict α -scattering differential cross sections. Since the reaction parameters are fixed in the case of ^{40}Ca , these predictions do not involve any adjustable parameters. The important calcium isotope family has been widely studied by electron scattering, μ and π mesic x rays, and hadron scattering experiments. For a summary of these results see Refs. 7, 17, and 18.

For ^{48}Ca the α -scattering predictions are compared to experimental data in Fig. 3. It can be seen that there is a tendency for the diffraction patterns resulting from the ^{48}Ca DME density to peak at smaller angles than the data, reflecting a slightly larger size. This tendency is noticeable at all three energies, although the disagreement is largest for the 42 MeV data. Overall, the cross section predictions derived from DDHF densities are more con-

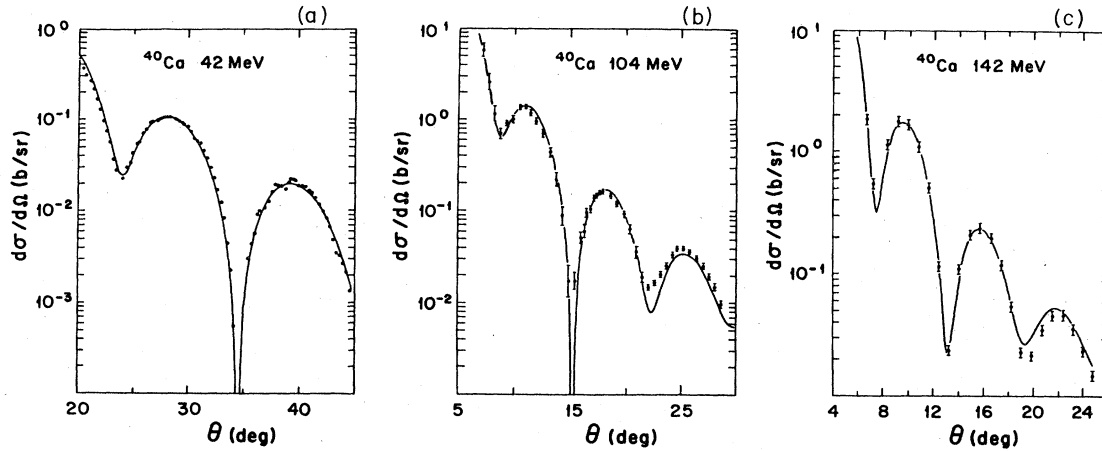


FIG. 2. Fits for our calibration nucleus ^{40}Ca obtained using an energy independent range parameter for (a) 42 MeV, (b) 104 MeV, and (c) 142 MeV.

sistent with the data. These differences correspond to a radius difference of approximately 0.1 fm, of the same magnitude of our estimated model error. The present uniform treatment of all available data removes any inconsistencies due to the different procedures used in the original analysis. In the original analysis of the 104 MeV data the full angular range was used,¹⁴ while in the case of 42 MeV (Ref. 7) and 79 MeV (Ref. 15) data only the diffraction region was considered. It is not clear whether the small differences seen between data sets and the predictions are due to experimental error or inaccuracies in the reaction calculation. Given the importance of ^{48}Ca we feel that it would be useful to measure the $^{48}\text{Ca}/^{40}\text{Ca}$ cross sections at several energies in the same laboratory to

minimize systematic error.

In Fig. 3 calculations are shown with an empirical ^{48}Ca density. For the Ca isotopes these have been defined as

$$\rho_A(r) = \rho_{40}(r) + \Delta\rho_p(r) + \Delta\rho_n(r), \quad (3)$$

where $\rho_{40}(r)$ is a HF density for ^{40}Ca , $\Delta\rho_p(r)$ is the proton density difference obtained through electromagnetic interactions,¹⁸ and $\Delta\rho_n(r)$ is the neutron density difference obtained from an analysis of 800 MeV proton scattering.¹⁹ Since $\Delta\rho_n \gg \Delta\rho_p$, the use of the empirical density is a consistency check between the 800 MeV proton results, for which the interaction is almost isoscalar, and those for the α particle. As can be seen in Fig. 3, the results using the empirical density are almost indistinguishable from those

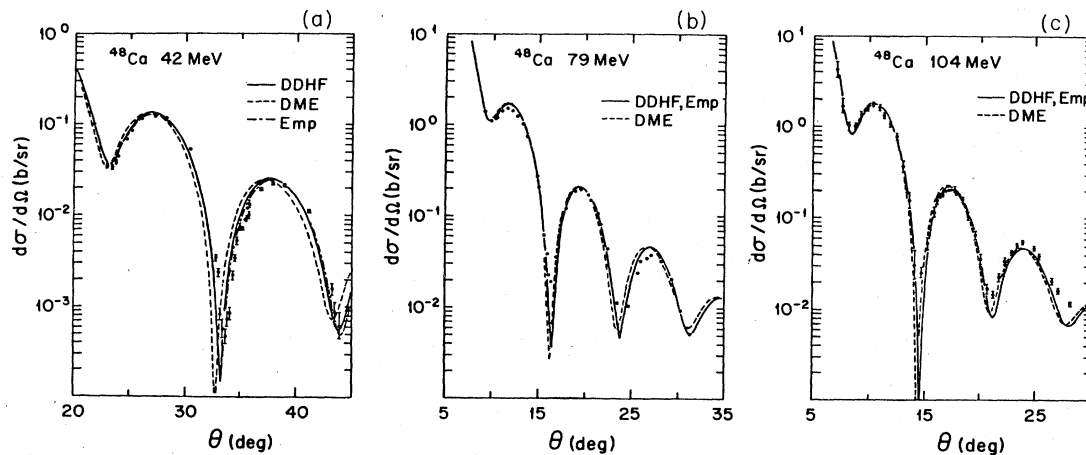


FIG. 3. Predicted differential cross section for ^{48}Ca at (a) 42 MeV, (b) 79 MeV, and (c) 104 MeV. The solid and dashed curves represent the predictions derived using the DDHF densities of Decharge-Gogny (Ref. 1) and the DME densities of Vautherin-Negele (Ref. 2), respectively. The prediction based on empirical densities (Emp) obtained from proton and electron scattering data is shown as a dashed-dot curve in part 3(a). For parts (b) and (c) the predictions using empirical densities are indistinguishable from the DDHF (Ref. 1) prediction.

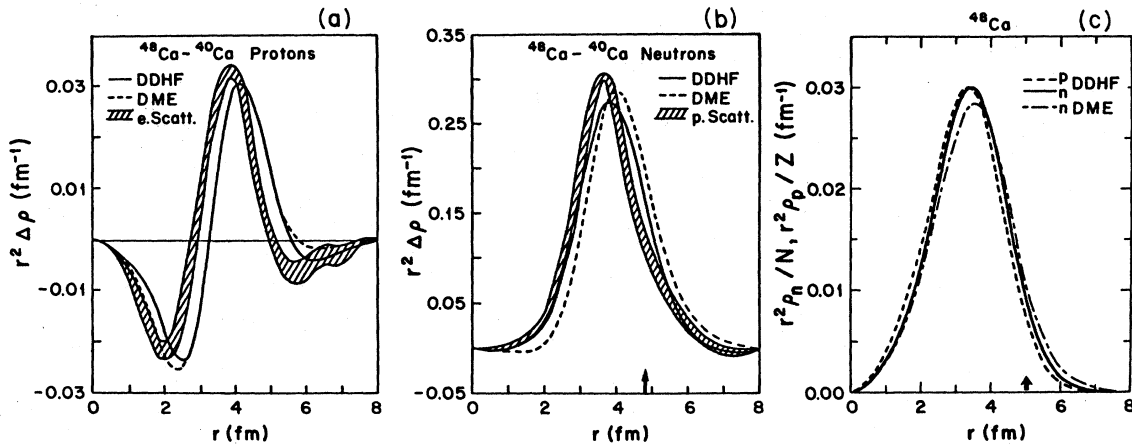


FIG. 4. ^{40}Ca densities. Parts (a) and (b) show the $^{48,40}\text{Ca}$ density differences for protons and neutrons, respectively. The curves are the DDHF predictions of Decharge and Gogny (Ref. 1) and the DME predictions of Vautherin and Negele (Ref. 2). The empirical results, shown with error bands, are from μ meson x rays and electron scattering for the proton densities (Ref. 18) and 800 MeV proton scattering (Ref. 19) for the neutron densities. Part (c) shows the reduced densities $r^2\rho_n/N$ and $r^2\rho_p/Z$ for ^{48}Ca . The proton densities for the two calculations (Refs. 1 and 2) are almost equal, and only the DDHF result (Ref. 1) is shown. The arrows in parts (b) and (c) indicate the region of maximum sensitivity for diffraction scattering of α particles.

using the densities of Decharge and Gogny.

The $^{40,48}\text{Ca}$ matter density differences, $r^2\Delta\rho$, are shown in Fig. 4. The factor of r^2 emphasizes the surface region, for which our probe is most sensitive. In Figs. 4(a) and (b), the HF proton and neutron density differences are compared to electron scattering¹⁸ and 800 MeV proton scattering¹⁹ results, respectively. The most precise measurement is the one concerning the proton distribution, the result of a combined analysis of electron scattering and muonic x-ray measurements.¹⁸ In Fig. 4(a) the empirical result is compared to the predictions of DME and

DDHF, which are almost indistinguishable in the surface region. It is also evident that both theories yield charge distributions with slightly larger spatial extent than the empirical density. The inclusion of higher order effects to the Hartree-Fock density modifies the theoretical densities. The inclusion of random phase approximation (RPA) correlations²⁰ improves the agreement between the predicted and the empirical measurements. The influence of even higher order corrections²¹ (2p-2h) appears to further improve the already reasonably good agreement.

In Fig. 4(b) the isotopic neutron density difference for

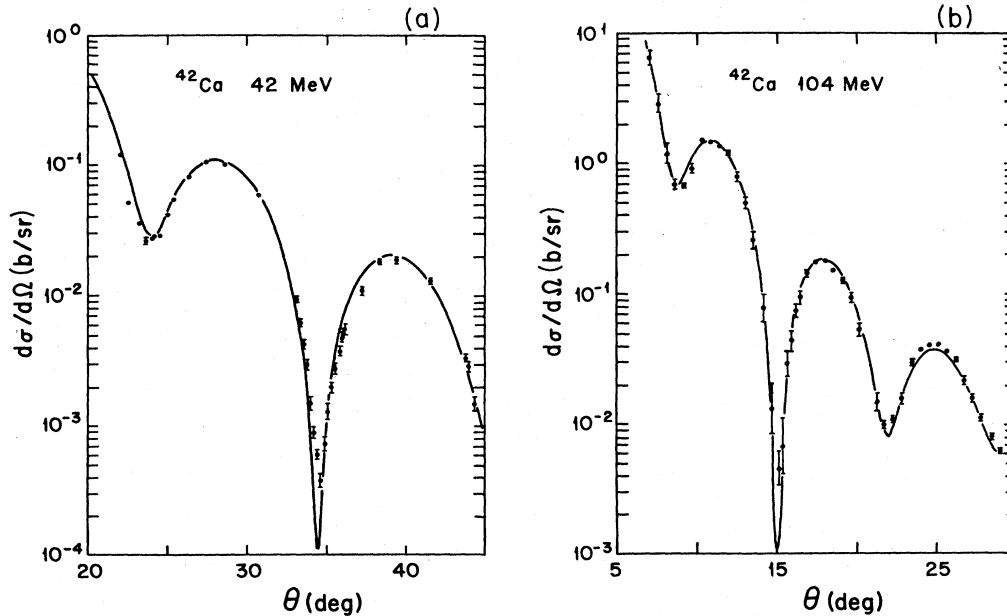


FIG. 5. Predictions of the differential cross section for ^{42}Ca based on the HF density of Decharge-Gogny for (a) 42 MeV and (b) 104 MeV.

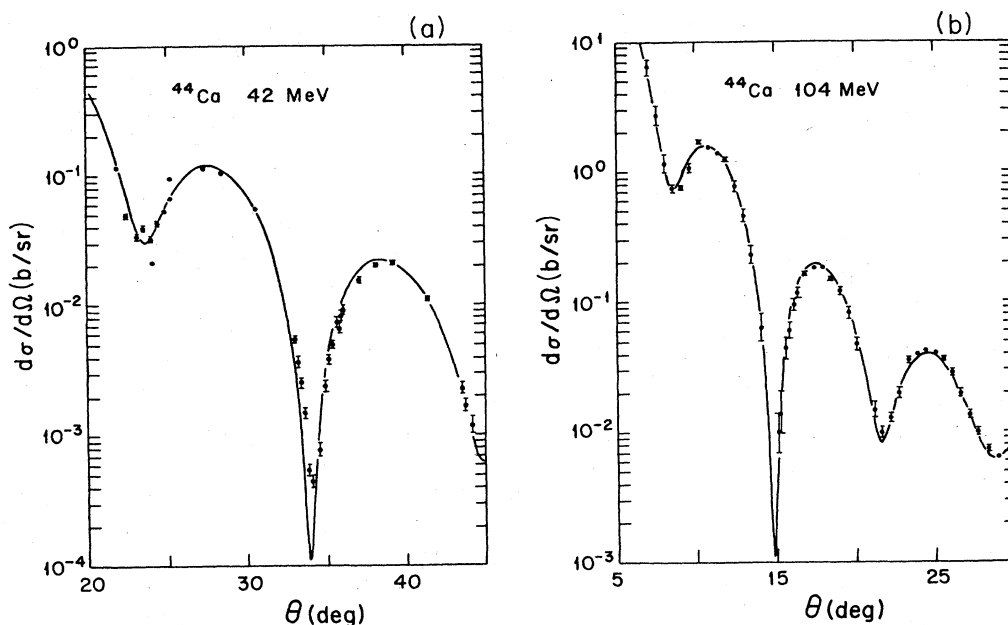


FIG. 6. Predictions for ^{44}Ca . Description is the same as that in Fig. 5.

$^{40,48}\text{Ca}$ is presented. The empirical neutron density has been obtained from the analysis of 800 MeV proton scattering data.¹⁹ It can be seen that this density is about ten times larger than the corresponding proton density and is the result of the addition of eight neutrons in the $f_{7/2}$ shell. As one might expect, the shape of the density has the qualitative features of an $f_{7/2}$ probability density. The difference between the two theoretical calculations in

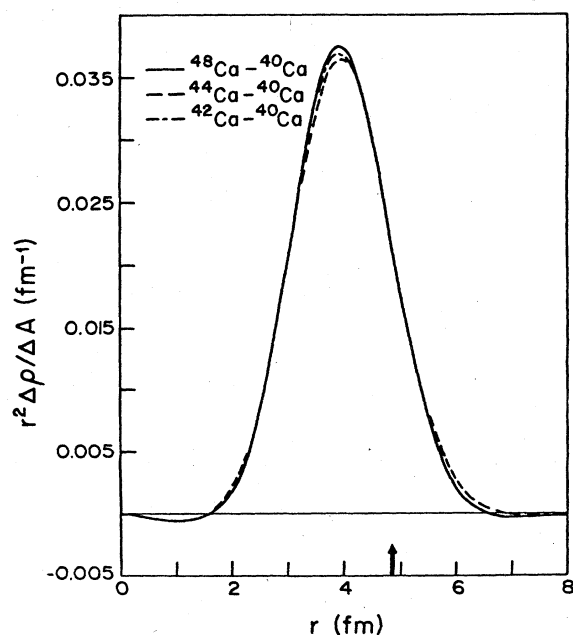


FIG. 7. Predicted isotopic density differences per nucleon for $^{48,44,42}\text{Ca}-^{40}\text{Ca}$ predicted by Decharge-Gogny. The arrow shows the region of maximum sensitivity of the α -particle projectiles.

this case is quite noticeable. The density of Negele and Vautherin extends beyond the empirical result by almost 0.3 fm. Unlike the density of Decharge and Gogny, it consistently lies outside the experimental error band.

The α probe, being isoscalar in nature, is equally sensitive to protons and neutrons (except for the trivial Coulomb correction). The α -scattering results will therefore reflect the qualitative features of the matter distribution which is presented in Fig. 4(c). The spatial region of maximum sensitivity for our probe (~ 4.8 fm) is indicated by an arrow. In this region the DME neutron density is larger than the DDHF. This noticeable difference results in a diffraction pattern that is shifted to smaller angles as was noted above (see Fig. 3).

The work presented here as well as the analysis of α -scattering data presented in an earlier paper⁷ favors the DDHF density of Decharge and Gogny for ^{48}Ca over the DME density of Vautherin-Negele. The DDHF theory yields a smaller rms radius, in agreement with this work and most other recent analyses of hadronic data. An extensive comparison to other hadronic probes and different analysis of the alpha scattering data has been presented in an earlier paper⁷ and will not be repeated here.

Using the theoretical densities of DDHF, predictions were made for ^{42}Ca and ^{44}Ca that match the available experimental measurements at 42 and 104 MeV. They are shown in Figs. 5 and 6. Again, as in the case of ^{48}Ca , the agreement with experiment is excellent.

The normalized density differences, $r^2\Delta\rho/\Delta A$, obtained from the Decharge-Gogny densities are shown in Fig. 7. They are derived from the same densities used in the calculated cross sections shown in Figs. 1, 2, 3, 5, and 6. We observe here the remarkable fact that the DDHF theory produces an almost perfect linear additive effect in the ground state matter distribution as the $f_{7/2}$ shell is being

closed. Equally important for this work is the observation that the region of maximum sensitivity, indicated by the solid arrow, lies very near the maximum of the isotopic difference distribution. Figure 7 thus provides another demonstration of the fact that elastic alpha scattering is a particularly sensitive probe of isotopic growth.

IV. CONCLUSIONS

The comparison of elastic alpha scattering data to those predicted using a double folding model and Hartree-Fock densities allows the evaluation of the ability of Hartree-Fock theories in accurately predicting isotopic growth. The accuracy of this comparison is primarily due to two factors: (a) only the diffraction scattering regime is considered, a region which can easily yield size information and where multistep processes are small and (b) only quantities relative to ^{40}Ca are being extracted. The normalization to ^{40}Ca is important, not only because it connects our results to a well-studied and rather well-understood nucleus, but mainly because it allows all the effects of the poorly understood reaction mechanism (non-locality, density dependence, etc.) to be absorbed in the pa-

rameters of the model. This model can be utilized to study the surface region of other isotopes.

The cross sections predicted using the Hartree-Fock densities of Decharge and Gogny¹ for $^{42,44,48}\text{Ca}$ are in excellent agreement with experimental data. Use of the Hartree-Fock DME ^{48}Ca density of Negele and Vautherin² results in predictions that do not agree as well with the data. This discrepancy is attributed to the larger (than the empirical and DDHF) neutron density predicted by DME [see Fig. 4(b)]. The results reported here are consistent with conclusions reached earlier in a similar analysis of alpha scattering data,^{7,15} as well as in a number of other hadronic reactions.^{7,19}

ACKNOWLEDGMENTS

We are indebted to Dr. J. Decharge and Dr. D. Gogny for many useful discussions and for making their calculations available prior to publication. We would like to thank Dr. B. Frois and Dr. L. Ray for useful discussions and for communicating their results and details of their analysis. This work was supported in part by the U.S. Department of Energy and the National Science Foundation under Contract Numbers DE-AC02-76ER03069 and NSF PHY 83-11717.

*Present address: Raytheon Company, Waltham, MA.

¹J. D. Decharge and D. Gogny, *Phys. Rev. C* **21**, 1568 (1980).

²J. W. Negele and Vautherin, *Phys. Rev. C* **5**, 1472 (1972).

³J. L. Friar and J. W. Negele, *Advances in Nuclear Physics* (Plenum, New York, 1975), Vol. 8.

⁴J. M. Cavedon, Ph.D. thesis, University of Paris, 1981 (unpublished).

⁵B. Frois, in *Intermediate Energy Nuclear Physics*, Proceedings of the International School of Intermediate Energy Nuclear Physics, edited by R. Bergere, S. Costa, and C. Schaerf, (World Scientific, Singapore, 1982), p. 61; Proceedings of the International Conference on Nuclear Physics, Florence, Italy, 1983, edited by P. Blasi and R. A. Ricci, Vol. 2.

⁶A. W. Thomas, in *Proceedings of the International Conference on Nuclear Physics, Berkeley, 1980*, edited by R. M. Diamond and J. O. Rasmussen (North-Holland, Amsterdam, 1981).

⁷C. N. Papanicolas, W. Q. Sumner, J. S. Blair, and A. M. Bernstein, *Phys. Rev. C* **25**, 1296 (1982).

⁸A. M. Bernstein and W. A. Seidler, *Phys. Lett.* **34B**, 569 (1971); **39B**, 583 (1972).

⁹C. G. Morgan and D. F. Jackson, *Phys. Rev.* **188**, 1758 (1969); D. F. Jackson, *Phys. Lett.* **32B**, 233 (1970); C. J. Batty, E.

Friedman, and D. F. Jackson, *Nucl. Phys.* **A175**, 1 (1971); J. S. Lilley, *Phys. Rev. C* **3**, 2229 (1971).

¹⁰G. M. Lerner, J. C. Hiebert, L. L. Rutledge, and A. M. Bernstein, *Phys. Rev. C* **6**, 1254 (1972).

¹¹H. Feshbach, *Annu. Rev. Nucl. Sci.* **8**, 49 (1958).

¹²A. M. Bernstein, in *Advances in Nuclear Physics*, edited by M. Baranger and E. Vogt (Plenum, New York, 1969), Vol. 3.

¹³B. Sinha, *Phys. Rep.* **C1**, 20 (1975).

¹⁴H. L. Gils, E. Friedman, Z. Majka, and H. Rebel, *Phys. Rev. C* **21**, 1245 (1980).

¹⁵G. M. Lerner, J. H. Hiebert, L. Rutledge, C. N. Papanicolas, and A. M. Bernstein, *Phys. Rev. C* **12**, 778 (1975).

¹⁶D. A. Goldberg, S. M. Smith, and G. F. Burdzit, *Phys. Rev. C* **10**, 1362 (1975).

¹⁷Proceedings of the Karlsruhe International Discussion Meeting, edited by H. Rebel, H. J. Gils, and G. Schratz, Kernforschungszentrum, Karlsruhe Report KFK 2830, 1979.

¹⁸H. J. Emrich *et al.*, *Nucl. Phys.* **A369**, 401c (1983).

¹⁹L. Ray, *Phys. Rev. C* **23**, 828 (1981).

²⁰D. Gogny, private communication.

²¹M. Waroquier, J. Bloch, G. Wenes, and K. Heyde, *Phys. Rev. C* **28**, 1791 (1983).